DOI: 10.1002/ejic.200501121

Rational Design and Control of the Dimensions of Channels in Three-Dimensional, Porous Metal-Organic Frameworks Constructed with Predesigned Hexagonal Layers and Pillars

Cui-Jin Li,[a] Sheng Hu,[a] Wei Li,[b] Chi-Keung Lam,[a] Yan-Zhen Zheng,[a] and Ming-Liang Tong*[a]

Keywords: Cobalt / Microporous / MOFs / Imidazole-4,5-dicarboxylate / Pillar / Magnetism

New three-dimensional, microporous metal-organic frameworks exhibiting reversible water adsorption, constructed from hexagonal $[Co_3(imda)_2]$ layers and *N*,*N*′-pillars, in which the dimensions of the channels are rationally adjustable by varying the lengths of pillars, have been designed, hydrothermally synthesized, and characterized.

Introduction

Pillared metal-organic framework (MOF) structures, analogous to natural clays and zeolites, are potentially important for applications in adsorption, separation and catalysis.[1,2] Although many attempts have been made to prepare functionalized pillared materials through cross-linking metal-phosphate, metal-phosphonate, or metal-sulfonate layers,[1a] these structures are built upon closed-window layers and pillars.[1,2] Contrasting the metal-phosphate, -phosphonate or -sulfonate systems, we have, with the aid of crystal engineering, been recently investigating rational synthetic strategies towards designed assembly of microporous MOFs constructed from the cationic layers with "open windows" and anionic linear dicarboxylates as pillars.[3] The advantage of this synthetic method promises not only to produce a wide variety of porous MOF materials with controlled channel sizes but also to mediate their chemical behavior by the decoration of diverse functional groups as part of the pillars. Recently, imidazole-4,5-dicarboxylic acid ($imdaH_3$) has been used as a versatile ligand to construct some intriguing porous MOFs, such as the molecular square[4a] and cube[4b,4c] in $Na_2[Co_4(imda)_4(2,2'\text{-bpy})]$ and $[Ni_8(imdaH)_{12}]^{8-}$, respectively. Among the coordination modes of the $imda^{3-}$ ligand in the reported complexes, the most remarkable one is the triangular arrangement of the three metal ions around $imda^{3-}$ (Scheme 1), which implies that it can be employed as a module in the construction of hexagonal layers by sharing the corners of the trigonal subunit $[M_3(imda)_2]$. In this communication, we report a strategy for pillaring the hexagonal $[M_3(imda)_2]$ layers into three 3D, porous MOF solids with controlled channel sizes (Scheme 2): $[Co_3(imda)_2(pyz)_3]\cdot 8H_2O$ (**1**), $[Co_3(imda)_2(4,4'\text{-bpy})_3]\cdot 4,4'\text{-bpy}\cdot 8H_2O$ (**2**), and $[Co_3(imda)_2(2,5\text{-bptz})_3]\cdot 2,5\text{-bptz}\cdot 9H_2O$ (**3**) [pyz = pyrazine, 4,4′-bpy = 4,4′-bipyridine, 2,5-bptz = 2,5-bis(pyrid-4-yl)-1,3,4-thiadiazole].

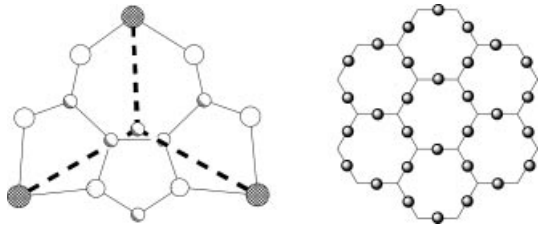

Scheme 1. Predesigned hexagonal layer constructed from the 3-connected 4,5-imda ligand.

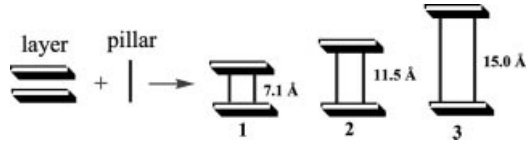

Scheme 2. A strategy for design and control of the channels in **1**–**3**.

Results and Discussion

Hydrothermal reactions of $CoCl_2\cdot 6H_2O$, $imdaH_3$, NaOH, and different *N*,*N*′-pillars (pyz, 4,4′-bpy, or 2,5-bptz) in a mol ratio of 1.5:1:3:1.5 generate crystals of **1**–**3**.

[a] State Key Laboratory of Optoelectronic Materials and Technologies, Institute of Optoelectronic and Functional Composite Materials & School of Chemistry and Chemical Engineering, Sun Yat-Sen University,
Guangzhou 510275, China
Fax: +86-20-8411-2245
E-mail: tongml@mail.sysu.edu.cn
[b] Department of Chemistry, Hanshan Teacher's College, Chaozhou, Guangdong 521041, China
Supporting information for this article is available on the WWW under http://www.eurjic.org or from the author.

Single-crystal X-ray analysis has revealed that **1** crystallizes in the hexagonal space group *P6/mmm*. The Co^{II} ions occupy Wyckoff position 3(*f*) with site symmetry *mmm*. Notably, the ideal molecular symmetries of the pyz ligand (D_{2h}) and the imda trianion (C_{2v}) are retained in the crystal structure, but the imda trianion exhibits a threefold disorder about the $\bar{6}$-axis (Figure S1). The Co^{II} ions are located in two different distorted octahedral coordination environments, $[CoO_2N_4]$ or $[CoO_4N_2]$ (Figure 1a). The coordination sphere is formed by four N atoms (two from pyz and two from imidazolate) and two carboxylato O atoms, or by two pyridyl N atoms and four carboxylato O atoms [Co–N_{imda} = 1.955(13), Co–N_{bpy} = 2.162(12), Co–O = 2.193(15) Å]. Each imda ligand bridges three Co atoms [Co···Co separations of 6.091(4) Å] to generate neutral and essentially planar $[Co_3(imda)_2]$ layers with (6,3) topology (Figure 2a). For simplicity, one of three possible orientations of $imda^{3-}$ is considered. Each 2D layer consists of two types of hexagonal 24-membered rings: Co_6(imidazolato)$_6$ and Co_6(carboxylato)$_6$. Interestingly, each Co_6(imidazolato)$_6$ ring is surrounded by six Co_6(carboxylato)$_6$ rings, while each Co_6(carboxylato)$_6$ ring is alternately surrounded by three Co_6(imidazolato)$_6$ rings and three Co_6(carboxylato)$_6$ rings. A sixfold axis lies across each cavity of the hexagonal layer. It is noteworthy that the hexagonal $[Co_3(imda)_2]$ layers are ideally stacked in an AAA fashion along the *c*-axis and are further pillared by pyz spacers into a non-interpenetrated 3D microporous MOF structure with the effective channel size of 4.7 × 4.7 Å estimated from the van der Waals radii for carbon (1.70 Å), hydrogen (1.20 Å),

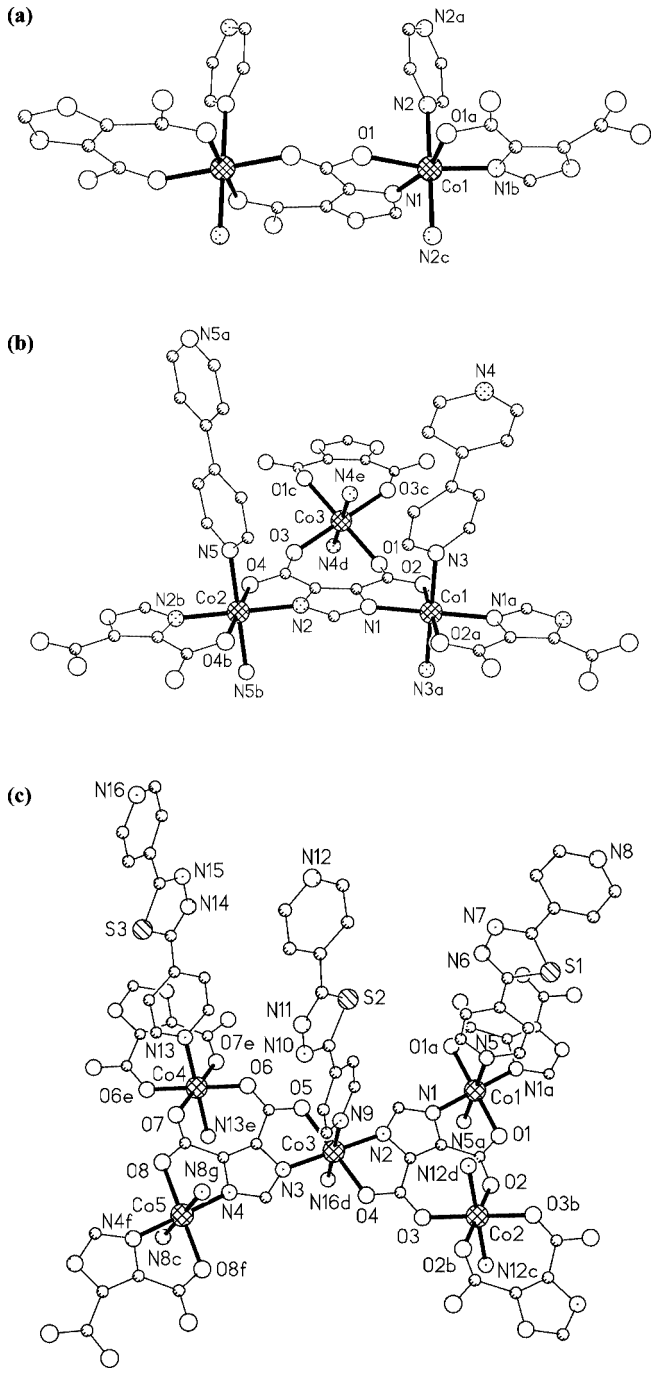

Figure 1. Coordination geometries of the Co^{2+} ions in **1** (a), **2** (b), and **3** (c).

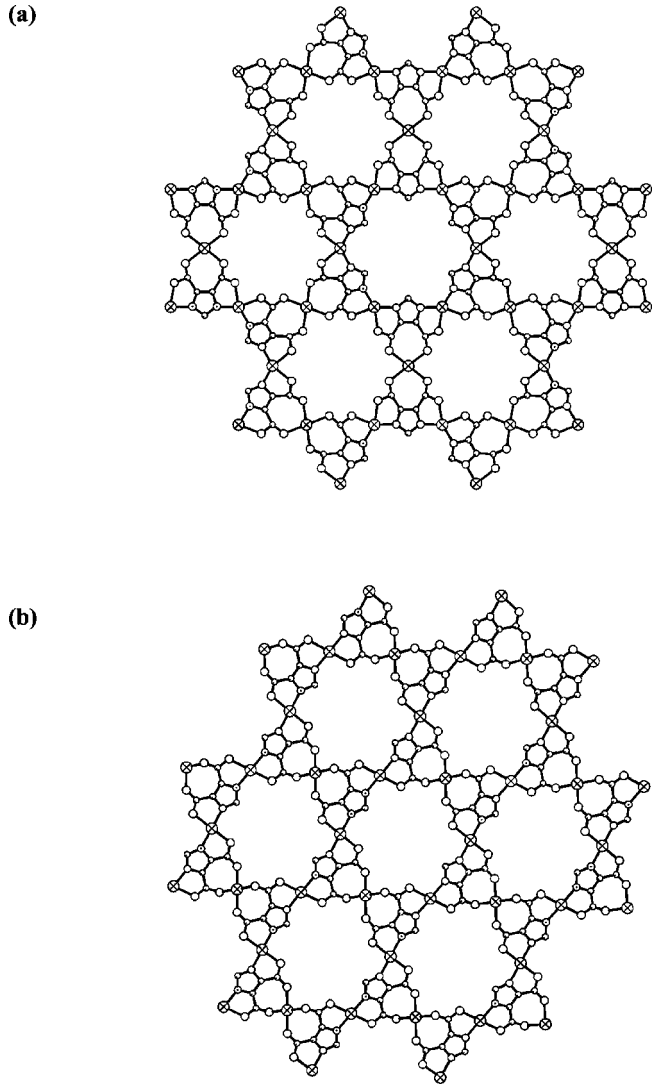

Figure 2. 2D hexagonal layers in **1** (a), and **2** or **3** (b).

nitrogen (1.55 Å), and oxygen (1.40 Å) (Figure S2 and Figure 3a). The disordered guest water molecules are located within these channels. An analysis with PLATON[5] suggested that the channels occupy 39.1% of the crystal volume. The network topology can be simplified by considering just the cobalt atoms (represented by a square-planar node) and the tri-connected imda ligands (represented by a triangular node); the bidentate pyz ligands can be represented simply as links between the cobalt nodes. The resulting net, shown in Figure 3b, is a rare 3D (3,4)-connected net with triangular and square-planar nodes in the ratio 2:3. A topological analysis of this net was performed with OLEX.[6] The long topological (O'Keeffe) vertex symbol is $6_2.6_2.6_2.6_2.12_2$ for the Co node and $6_2.6_2.6_2$ for the imda node, giving the short vertex symbol $(6^3)_2(6^4.8.10)_3$. The net is different to other previously identified (3,4)-connected networks.[7]

The porous MOF structures of **2** and **3** are similar to that of **1**. Both of them are built of neutral hexagonal $[Co_3(imda)_2]$ layers and longer 4,4′-bpy or 2,5-bptz pillars. The asymmetric unit of **2** contains one and a half 4,4′-bpy ligand, one $imda^{3-}$ ion, and three independent Co^{II} ions lying at inversion centers (Figure 1b). Both Co1 and Co2 atoms are similarly in a distorted octahedral $[CoO_2N_4]$ environment, in which the coordination sphere for Co1 or Co2 is formed by two pyridyl N atoms, two imidazolate N atoms, and two carboxylate O atoms [Co–N_{imda} = 2.046(3)–2.048(4), Co–N_{bpy} = 2.172(4)–2.206(3), Co–O = 2.106(3)–2.119(3) Å], while the coordination sphere for Co3 is formed by two pyridyl N atoms and four carboxylato O atoms [Co–N = 2.157(3), Co–O = 2.063(3)–2.066(3) Å]. Each imda ligand bridges three Co atoms with Co···Co separations of 5.7704(5)–6.2939(4) Å. For **3**, the asymmetric unit of the host MOF contains five unique Co^{II} atoms, four (Co1, Co2, Co4, and Co5) of which lie across inversion centers and the other one (Co3) on a general position, two imda ligands which lie on general positions, and three unique 2,5-bptz ligands (Figure 1c). The adjacent intralayer Co···Co distances separated by the imda ligands are 5.8168(9)–6.3064(9) Å.

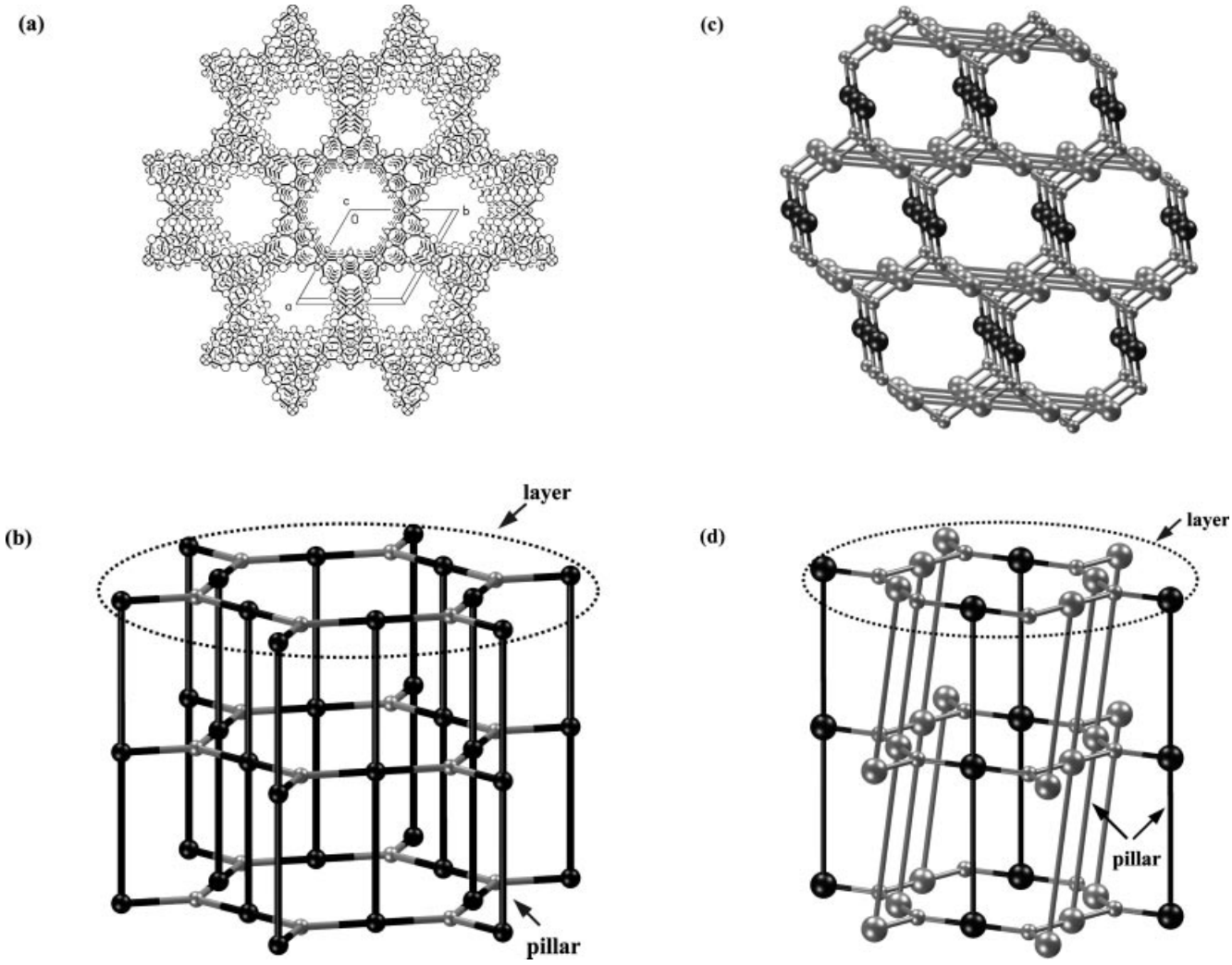

Figure 3. (a) The pillared 3D MOF in **1**. (b) Topological connectivity in **1**. (c) Topological net of the pillared 3D MOF in **2** or **3**. (d) Topological connectivity in **2** or **3**. The big dark grey or black spheres represent cobalt atoms, while the small grey spheres represent the centers of mass of imda ligands. The *N*,*N*′-pillar ligands are represented by interlayer bold lines.

In contrast to that in **1**, each 2D hexagonal layer in **2** or **3** consists of only hexagonal Co_6(imidazolato)$_2$(carboxylato)$_4$ 24-membered rings (Figure 2b). Adjacent hexagonal layers are stacked in a ABAB fashion and are further pillared by 4,4′-bpy or 2,5-bptz spacers into a non-interpenetrated 3D microporous MOF structure with the effective channel sizes of 4.2×6.2 Å and 4.7×6.5 Å for **2** and **3**, respectively. It should be noted that the network topology of **2** and **3** are identical, but different from that of **1** though the three 3D MOF structures are 3D (3,4)-connected nets with triangular and square-planar nodes in the ratio 2:3. In **1**, all the Co nodes are the same. But in **2** and **3**, only two-thirds of the Co nodes are equivalent (for **2**: Co1 and Co3; for **3**: Co1, Co2, Co4 and Co5). The difference between the two types of nodes can be seen in Figure 3c, d. The long topological (O'Keeffe) vertex symbol is $6_2.6_2.6.6.12_2.12_2$ and $6.6.6.6.10_2$ for the two kinds of Co nodes, and $6.6.6_2$ for the imda node, giving the short vertex symbol $(6^3)_2(6^4.8^2)_2$-$(6^4.10^2)$. An analysis with PLATON[5] suggested that the channels occupy 38.8% and 44.6% of the crystal volume for **2** and **3**, respectively. The guest 4,4′-bpy/2,5-bptz and water molecules are located within these channels. The calculated crystal densities (in the absence of guests) of 1.172 g cm^{-3} and 1.09 g cm^{-3} are comparable to those found for some porous MOF materials with low density.[8]

To examine the thermal stability of these porous networks, thermal gravimetric (TG) analyses and powder X-ray diffraction (XRD) measurements were carried out. The thermal decomposition behaviors of **1**, **2**, and **3** are much alike. For **1**, the first weight loss of 15.7% from 20 to 180 °C is in accordance with the loss of eight lattice water molecules per Co_3 (calculated: 16.6%), while the release of the pyz and imda components occurs at ca. 250 °C and 360 °C in two separate steps (Figure S4) to yield the residue Co_3O_4 at ca. 410 °C (found: 28.6%; calculated: 27.8%). The TG curve of **2** indicate the release of all lattice water molecules before 106 °C (found: 11.3%; calc: 11.5%). At 265 °C, the solvated 4,4′-bpy and coordinated ligands start to be released (Figure 4). No chemical decomposition was observed between 106 and 265 °C. The TG curves of the dehydrated and rehydrated samples of **2** show that it exhibits reversible water adsorption. Powder XRD patterns of **2** and dehydrated samples of **2** are nearly identical, indicating that the initial framework is retained after the lattice water molecules are removed by heating at 180 °C under vacuum for 8 h. For **3**, the first weight loss of 9.9% from 20 to 120 °C is in accordance with the loss of nine lattice water molecules per Co3 (calculated: 10.1%). No chemical decomposition was observed between 120 and 350 °C (Figure S6). Similar reversible dehydration and rehydration are also found for **1** and **3** (Figures S4–6).

The temperature-dependent magnetic susceptibility, χ_M, of **1**, **2**, and **3** were measured in a 5.0-kOe field (Figure S7). At room temperature, $\chi_M T$ is 8.30, 8.29, and 7.20 cm^3 mol^{-1} K per Co_3 unit for **1**, **2**, and **3**, respectively, which is significantly higher than the spin-only value (5.63 cm^3 mol^{-1} K) expected for three uncoupled Co^{II} ions (S = 3/2), indicating that the orbital contribution is incompletely quenched. Upon cooling, the $\chi_M T$ gradually decreases owing to the contribution of single-ion behavior of high-spin Co^{II} ions and also to antiferromagnetic exchange between the Co centers. The $\chi_M(T)$ in the high-temperature region (30–280 K) can be fit into the Curie–Weiss equation with C = 9.77 cm^3 mol^{-1} K and θ = –53.99 K for **1**, C = 9.69 cm^3 mol^{-1} K, and θ = –46.24 K for **2** and C = 8.48 cm^3 mol^{-1} K and θ = –58.94 K for **3**; these values agree well with those expected for high-spin Co^{II} ions in octahedral sites.[9a] The negative sign of θ and the decrease of χT point to the existence of antiferromagnetic exchange interactions. Spin-orbit coupling most certainly also contributes to this decay.[9a–9c] Detailed magnetic studies and other functions of this porous family are under way.

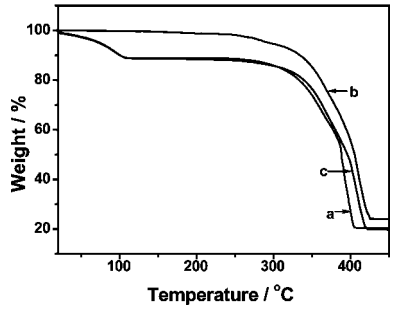

Figure 4. TG data for **2**: (a) as-synthesized sample, (b) dehydrated sample at 180 °C, (c) re-hydrated sample.

In conclusion, we present a new strategy for the generation of novel 3D porous metal-organic framework solids that exhibit reversible water adsorption with predesigned hexagonal [Co_3(imda)$_2$] layers and length-controllable N,N'-spacers as pillars. They may be good candidates for porous materials owing to their high thermal stability and reversible guest exchange.

Experimental Section

X-ray Crystallographic Study: Diffraction intensities of **1**, **2**, and **3** were collected with a Bruker Apex CCD area-detector diffractometer (Mo-K_α, λ = 0.71073 Å). Absorption corrections were applied by using the multiscan program SADABS.[10] The structures were solved with direct methods and refined with a full-matrix least-squares technique with the SHELXTL program package.[11]

Crystal and structure-refinement parameters. Compound **1**: $C_{22}H_{30}Co_3N_{10}O_{16}$, M = 867.35, hexagonal, space group *P6/mmm* (No. 191), a = 12.183(1), c = 7.092(1) Å, V = 911.6(2) Å^3, Z = 1, T = 123(2) K, F(000) = 441, D_c = 1.580 g cm^{-3}, μ(Mo-K_α) = 1.427 mm^{-1}; R_1 = 0.0847, wR_2 = 0.1687 and GOF = 1.159 for 61 parameters, 307 reflections with $|F_o| \geq 4\sigma(F_o)$. Compound **2**: $C_{50}H_{50}Co_3N_{12}O_{16}$, M = 1251.81, triclinic, space group $P\bar{1}$ (No. 2), a = 11.448(1), b = 11.541(1), c = 11.766(1) Å, α = 65.370(1), β = 80.540(1) γ = 72.759(1)°, V = 1348.2(2) Å^3, Z = 1, T = 123(2) K, F(000) = 663, D_c = 1.542 g cm^{-3}, μ(Mo-K_α) = 0.993 mm^{-1}; R_1 = 0.0580, wR_2 = 0.1552 and GOF = 1.036 for 412 parameters, 4147 reflections with $|F_o| \geq 4\sigma(F_o)$. Compound **3**: $C_{58}H_{52}Co_3N_{20}O_{17}S_4$, M = 1606.23, triclinic, space group $P\bar{1}$ (No. 2), a = 11.791(1), b = 17.050(2), c = 20.795(2) Å, α = 104.726(2), β = 106.360(2), γ = 103.481(2)°, V = 3664.6(7) Å^3, Z = 2, T = 123(2) K, F(000) = 1642,

D_c = 1.456 g cm^{-3}, μ(Mo-K_α) = 0.862 mm^{-1}; R_1 = 0.0834, wR_2 = 0.2467 and GOF = 1.029 for 955 parameters, 7210 reflections with $|F_o| \geq 4\sigma(F_o)$. The PLATON SQUEEZE procedure[12] was also used to treat regions of disordered solvent in **2** which could not be sensibly modeled in terms of atomic sites. Their contribution to the diffraction pattern was removed and modified F_o^2 written to a new HKL file. The number of electrons thus located, 160.1 per unit cell, is included in the formula, formula weight, calculated density, μ, and F(000). This residual electron density was assigned to eight water molecules and a 4,4′-bpy [8 × 10 (H_2O) + 1 × 82 (4,4′-bpy) = 162e]. However, the disordered solvents in **1** and **3** could not be subtracted from the corresponding diffraction patterns by the squeeze/bypass procedure because of their disordered host MOF structures.

CCDC-289570 (**1**), CCDC-284833 (**2**) and CCDC-284834 (**3**) contain the supplementary crystallographic data for this paper. These data can be obtained free of charge from The Cambridge Crystallographic Data Centre via www.ccdc.cam.ac.uk/data_request/cif.

Supporting Information (see footnote on the first page of this article): X-ray crystallographic files of **1**–**3** (CIF), synthesis, packing plots, TG curves, simulated and experimental powder XRD data, temperature- and field-dependent magnetic susceptibility of **1**–**3**.

Acknowledgments

We thank Dr. S. R. Batten for his helpful discussions about the topology. This work was supported by the National Science Funds for Distinguished Young Scholars of China (No. 20525102), the NSFC (20471069), the FANEDD of China (200122), and the Scientific and Technological Project of Guangdong Province (04205405).

[1] a) A. Clearfield, Z. Wang, *J. Chem. Soc., Dalton Trans.* **2002**, 2937; b) S. Kitagawa, R. Kitaura, S.-i. Noro, *Angew. Chem. Int. Ed.* **2004**, *43*, 2334; c) B. F. Hoskins, R. Robson, *J. Am. Chem. Soc.* **1990**, *112*, 1546; d) M. Eddaoudi, D. B. Moler, H. Li, B. Chen, T. M. Reineke, M. O'Keeffe, O. M. Yaghi, *Acc. Chem. Res.* **2001**, *34*, 319; e) P. J. Hagrman, D. Hagrman, J. Zubieta, *Angew. Chem. Int. Ed.* **1999**, *38*, 2638; f) C. Janiak, *Dalton Trans.* **2003**, 2781.

[2] a) *Pillared Layered Structures: Current Trends and Applications* (Ed.: I. V. Mitchell), Elsevier, London, **1990**; b) L. Pan, B. S. Finkel, X. Huang, J. Li, *Chem. Commun.* **2001**, 105.

[3] a) S.-L. Zheng, M.-L. Tong, R.-W. Fu, X.-M. Chen, S. W. Ng, *Inorg. Chem.* **2001**, *40*, 3562; b) S.-L. Zheng, M.-L. Tong, X.-M. Chen, *Coord. Chem. Rev.* **2003**, *246*, 185.

[4] a) C.-F. Wang, E.-Q. Gao, Z. He, C.-H. Yan, *Chem. Commun.* **2004**, 720; b) Y. Liu, V. Kravtsov, R. D. Walsh, P. Poddar, H. Srikanth, M. Eddaoudi, *Chem. Commun.* **2004**, 2806; c) R.-Q. Zou, L. Jiang, H. Senoh, N. Takeichia, Q. Xu, *Chem. Commun.* **2005**, 3526; d) T. K. Maji, G. Mostafa, H.-C. Chang, S. Kitagawa, *Chem. Commun.* **2005**, 2436; e) Y.-L. Wang, D.-Q. Yuan, W.-H. Bi, X. Li, X.-J. Li, F. Li, R. Cao, *Cryst. Growth Des.* **2005**; *5*, 1849; f) Y.-Q. Sun, J. Zhang, Y.-M. Chen, G.-Y. Yang, *Angew. Chem. Int. Ed.* **2005**, *44*, 5814; g) W.-G. Lu, C.-Y. Su, T.-B. Lu, L. Jiang, J.-M. Chen, *J. Am. Chem. Soc.* **2006**, *128*, 34; h) W.-G. Lu, L. Jiang, X.-L. Feng, T.-B. Lu, *Cryst. Growth Des.* **2006**, *6*, 564.

[5] A. L. Spek, *PLATON, A Multipurpose Crystallographic Tool*, Utrecht University, Utrecht, The Netherlands, **2003**.

[6] O. V. Dolomanov, A. J. Blake, N. R. Champness, M. Schröder, *J. Appl. Crystallogr.* **2003**, *36*, 1283.

[7] a) B. F. Abrahams, S. R. Batten, H. Hamit, B. F. Hoskins, R. Robson, *Angew. Chem. Int. Ed. Engl.* **1996**, *35*, 1690; b) V. A. Blatov, L. Carlucci, G. Ciani, D. M. Proserpio, *CrystEngComm* **2004**, *6*, 377.

[8] a) O. M. Yaghi, M. O'Keeffe, N. W. Ockwig, H. K. Chae, M. Eddaoudi, J. Kim, *Nature* **2003**, *423*, 705; b) S. Hu, J.-C. Chen, M.-L. Tong, B. Wang, Y.-X. Yan, S. R. Batten, *Angew. Chem. Int. Ed.* **2005**, *44*, 5471.

[9] a) R. L. Carlin, *Magnetochemistry*, Springer, Berlin, **1986**; b) F. E. Mabbs, D. J. Machin, *Magnetism and Transition Metal Complexes*, Chapman and Hall, London, **1973**; c) E. Coronado, M. Drillon, P. R. Nugteren, L. J. De Jongh, D. Beltran, *J. Am. Chem. Soc.* **1988**, *110*, 3907.

[10] G. M. Sheldrick, *SADABS 2.05*, University Göttingen.

[11] *SHELXTL 6.10*, Bruker Analytical Instrumentation, Madison, Wisconsin, USA, **2000**.

[12] a) P. van der Sluis, A. L. Spek, *Acta Crystallogr., Sect. A* **1990**, *46*, 194; b) A. L. Spek, *Acta Crystallogr., Sect. A* **1990**, *46*, C34.

Received: December 19, 2005
Published Online: April 10, 2006

